

Assessment of embolization effect with temperature-sensitive p(N-isopropylacrylamide-co-butyl methylacrylate) nanogels in rabbit renal artery by CT perfusion and pathology

Zhen Zhang

Huazhong University of Science and Technology

Chunyuan Cen

Huazhong University of Science and Technology

Kun Qian

Huazhong University of Science and Technology

Han Li

Huazhong University of Science and Technology

Xin Zhang

Huazhong University of Science and Technology

Hongsen Zhang

Huazhong University of Science and Technology

Guina Ma

Huazhong University of Science and Technology

Yan Chen

Huazhong University of Science and Technology

Nanchuan Jiang

Huazhong University of Science and Technology

Chuansheng Zheng

Huazhong University of Science and Technology

Yanbing Zhao

Huazhong University of Science and Technology

Ping Han (✉ hanping_uh@hust.edu.cn)

Huazhong University of Science and Technology

Research Article

Keywords: p(N-isopropylacrylamide-co-butyl methylacrylate), (PIB), CT perfusion.

Posted Date: November 20th, 2020

DOI: <https://doi.org/10.21203/rs.3.rs-109516/v1>

License:  This work is licensed under a Creative Commons Attribution 4.0 International License.

[Read Full License](#)

Version of Record: A version of this preprint was published at Scientific Reports on March 1st, 2021. See the published version at <https://doi.org/10.1038/s41598-021-84372-w>.

Abstract

The temperature-sensitive *p*(N-isopropylacrylamide-co-butyl methylacrylate) (PIB) nanogel is a novel embolic agent, but methods to assess its performance are limited. The study aimed to assess the effect of embolization with PIB nanogels in rabbit renal artery by non-invasive computed tomography (CT) perfusion and pathology to evaluate the feasibility of the nanogel as a blood vessel embolization agent. Ten healthy adult Japanese rabbits underwent right renal arterial embolization with PIB nanogels. CT perfusion scans were performed pre- and post-treatment at different time points (1, 4, 8, and 12 weeks). Two rabbits were euthanized and histologically examined each time, and the remaining rabbits were sacrificed at 12 weeks after the embolization. The efficacy of the nanogels was further confirmed by pathological examination. The renal volume and renal blood flow of the right kidney significantly decreased post-treatment during the 12-week CT re-examination (both $P < 0.05$). No recanalization or collateral circulation was observed during this period for the PIB nanogel, which dispersed in blood vessels of all levels. The CT perfusion outcome showed changes in the kidneys similar to the pathological result. The embolic effect of PIB was good dispersion and permanency, and could be evaluated by non-invasive and quantitative CT perfusion.

Introduction

With the rapid development of interventional radiological technology, blood vessel embolism materials (including metal coils, anhydrous ethanol, Lipiodol, onyx, and Polyvinyl Alcohol (PVA)) have expanded the clinical indications, such as treatment of postpartum haemorrhage, gastrointestinal bleeding¹⁻³, preoperative embolotherapy of tumours^{4,5}, and embolization of vascular malformations⁶. However, the clinical application of these materials has some complications, such as spring coil or gel drop caused by obstructive nephropathy^{7,8}, ethanol embolism secondary pulmonary hypertension⁹, and high concentrations of onyx with neurotoxicity¹⁰; additionally, Lipiodol embolization is often incomplete or totally eradicated by tissue. Therefore, finding an effective method to solve the above problems is key.

Temperature-sensitive nanogels have gained considerable attention during the last decades because they undergo reversible and rapid volume phase transitions in response to changes in ambient temperature. First, these nanogels have good fluidity in fine catheters because they remain in the liquid solution state at a lower critical solution temperature (LCST). Second, their small size enables them to overcome some biological barriers. Furthermore, in situ formation could minimize trauma and ease the administration of nanogels as implants. In addition to good dispersibility and permanent embolism, the *p*(N-isopropylacrylamide-co-butyl methylacrylate) (PIB) nanogels made by our team has less inflammatory vascular response, better fluidity, and better operability than do PVA-embolized particles and Lipiodol^{11,12}.

Temperature-sensitive *p*(N-isopropylacrylamide-co-butyl methylacrylate) nanogels have been used as novel blood vessel embolic materials to solve the dilemma of peripheral artery embolization and permanent embolization¹¹⁻¹³. With the progress in preparation technology, materials have become more compatible and more convenient.

Some researchers have attempted to use digital subtraction angiography (DSA) to assess the long-term effect of embolization¹¹⁻¹⁴. However, a major drawback of DSA is invasion. Computed tomography (CT) perfusion imaging is a new, non-invasive technology that can provide data about renal morphological changes as well as quantified information of bilateral renal blood flow¹⁵.

In our previous study¹², PIB was first developed as a novel temperature-sensitive blood vessel embolic agent for addressing the dilemma of flowability and embolization in transarterial chemoembolization of hepatocellular carcinoma. The purpose of this study was to observe the feasibility of PIB as a blood vessel embolization agent through CT perfusion imaging and pathological examination, thus providing an experimental basis for the clinical application of a novel embolic agent.

Materials And Methods

Experimental materials

The visible embolization materials of the PIB nanogels demonstrated in this experiment were invented at the National Engineering Research Center for Nanomedicine, College of Life Science and Technology, Huazhong University of Science and Technology. PIB nanogels are new kinds of temperature-sensitive nanogels that can remain in a liquid state at a low temperature and become a gelatinous solid at temperatures above their LCST. Because it undergoes a transition from a flowable sol phase to a solidified gel phase at its LCST (35°C), the PIB nanogel is a liquid state at low temperature (25°C) and becomes a solid white gel at high temperature (37°C) (Fig. 1).

Study design

The experiment (n = 10) was designed to assess the dispersion of the PIB nanogel and to monitor its residue time. Rabbits were treated by right renal arterial embolization (RAE) with PIB nanogels and underwent CT perfusion pre- and post-treatment at different time points (1, 4, 8, and 12 weeks). Efficacy was confirmed by a pathological examination after CT perfusion.

Animal model preparation

Ten healthy adult Japanese long-eared white rabbits were provided by the experimental animal breeding plant of Tongji Medical College, Huazhong University of Science and Technology. The rabbits were aged 3–5 months, had body weights between 2.5 and 3 kg, and were in either gender. All procedures were reviewed and approved by the Institutional Animal Care and Use Committee at Tongji Medical College, Huazhong University of Science and Technology and are consistent with animal care guidelines.

Vascular embolization protocol

First, the animals fasted for 12 hours before each procedure. Sodium pentobarbital (2.0 wt.%, 30 mg/kg) was injected intravenously as anaesthesia. Then, interventional procedures were performed using a DSA unit with strict sterile technique. Finally, the right femoral artery was surgically isolated, and an 18-gauge

sheath needle was inserted. The PIB nanogels were injected into each rabbit with an average dose of 1.5 ml per rabbit (Fig. 2).

Perfusion CT

The parameters of the perfusion CT scanning and contrast agent injection are summarized in Table 1. A 320-detector row CT scanner (Aquilion One; Toshiba Medical Systems) was used in volumetric scan mode. A 22-gauge catheter was placed in the ear vein of the rabbit, and a nonionic contrast material (Iopamiron 350; Bayer HealthCare) was administered with a power injector (Ulrich CT Plus 150, Ulrich Medical). The scan area of the perfusion CT was set to cover at least both kidneys. During the scan, the rabbits were restrained and held still but were allowed to breathe. A rumpled towel was fixed against the subcostal abdominal wall of the rabbits using an elastic abdominal binder to minimize respiratory motion. Perfusion was calculated using the maximum slope model (Body Perfusion; Toshiba Medical System), and the results are shown in ml/min per 100 ml; additionally, the colour perfusion maps of renal blood flow (BF) were obtained.

Table 1. Parameters of perfusion CT

Parameters	
Scan parameters	
Number of detector rows	320
Craniocaudal coverage	160 mm
Collimation	0.5 mm
Tube voltage	80 kVp
Tube current	60 mA
Gantry rotation time	0.5 s
Matrix	512×512
Field of view	300 mm×350 mm
Contrast agent	
Iodine concentration	350 mg/mL
Total dose	3 mL
Injection rate	0.5 mL/s
Saline flush	8 mL with 0.5 mL/s
Scan	Every 2 s for 18 s
	Every 3 s for 15 s
	Every 7 s for 35 s
Note: The first scan was 6 s after initiating the contrast agent injection.	

Pathology

Macroscopic and microscopic pre- and post-RAE treatment

At different time points (1, 4, 8, and 12 weeks), the rabbits were euthanised after the CT perfusion was completed, and the kidneys were harvested for general pathological observation. Then, a coronal incision of the kidneys was performed, and a dividing ruler was placed next to the kidneys. Macroscopic observation was collected at each time point to note the size, shape, texture, colour, cortex, and medullary infarction of the right kidney after the RAE, in addition to observing the presence of any surviving kidney

tissue. The post-RAE renal tissues were fixed in 10% formalin for 48 hours, dehydrated in graded alcohol, and embedded in paraffin. Then, 4–5 μm sections were cut. The tissue samples were then stained with Masson's trichrome at different time points for evaluating ultrastructural changes and estimating the effects of the treatments.

Statistical analysis

Statistical analysis was performed using SPSS 20.0 and Microsoft Excel. The mean values and standard deviations are presented as ($\bar{x} \pm s$). Paired-samples *t* tests were used to assess the differences in the renal volume and BF in the right kidney pre- and post-treatment during the 12 weeks.

Results

Dispersion and permanency

During the arterial embolization procedure, all levels of renal arteries (large, small and peripheral) could be embolized with 2 mL of PIB nanogels by adjusting the injecting rate at 0.15 ml/s. This result implied that the PIB nanogels dispersed well in the blood vessels. A perfusion CT examination was performed to obtain the correlation quantitative index of paired renal volume and renal BF. These data showed that the right renal volume decreased and that the left side compensatorily increased. The right renal BF decreased to zero after the right RAE (Fig. 3). Significant differences were found in the renal volume ($P = 0.002$) and BF ($P = 0.001$) of the right kidney pre- and post-treatment during the 12 weeks. In addition, during the long-term follow-up CT examination, the right kidney showed no changes in BF reperfusion and revascularization after embolization (Fig. 4). In addition, the macro-pathological pictures (Fig. 5) of RAE at four different time points (1, 4, 8, and 12 weeks) showed that the right kidney gradually shrank after embolization, combined with the compensatory enlargement of the left kidney. At the first week, the embolized kidney was nearly yellowish white, and the renal medulla was ischaemic. At the fourth week, the embolized kidney was nearly yellow, the volume shrank, and the texture became hard, but the renal edge was yellowish white. At the eighth and twelfth weeks, the colour of the right kidney was pale, the volume was smaller, and the texture was harder. The calcification of the right renal tissue was observed. Distinguishing between the cortex and medulla was difficult, and no abscess was formed at last. The changes in the right renal volume between gross pathology and CT perfusion imaging were the same. All of these results indicated that PIB nanogel dispersion contributed to an effective embolization within 12 weeks. The histological results of the right kidney indicated that the nanogels were immobilized in the renal arteries and branches throughout the entire experimental period (Fig. 6). The renal cells and tissues maintained their intact structure and morphology at 1 week post-embolization, while oedema and coagulative necrosis occurred (a) and began to disintegrate at 4 weeks post-embolization (b). After embolization for 8 weeks, the pyknosis, rupture, dissolution and disappearance of renal cells indicated that PIB nanogel embolization resulted in an obvious embolic gangrene, and the gel was still in the blood vessels (c). The structure and morphology of the renal tissues were entirely destroyed, and significant calcifications were found at 12 weeks after embolization (d).

Discussion

In this study, we successfully performed embolization with PIB nanogels dispersion in rabbit renal arteries through CT perfusion scan and histological examinations before and after embolization.

Thermally-induced gelling systems have gained growing attention over the last decade. A smart polymer material can remain in a liquid solution state at LCST and become a gelatinous solid above LCST. With a transition temperature close to physiological temperature, smart polymer materials have been reported in blood vessel embolic materials^{13,16}, drug delivery¹⁷⁻¹⁹, precise cancer therapy^{20,21}, tissue engineering²², and cell sheet engineering^{23,24}. Most of the studies have focused on phase behaviour theory, drug delivery and promising biomedical applications. However, clinical follow-up of the treatment effect is equally important, and there are few animal experiments in this area.

The ideal vascular embolization material has the following characteristics: good dispersibility, radiopacity, biocompatibility and embolism permanency^{16,25}. Recently, gel performance has been greatly improved over the past decades, in terms of the viscosity, safety, radiopacity, phase transition temperature. In previous studies, PIB nanogels were confirmed to be nonadhesive, controllable, and not likely to cause severe inflammatory reactions of the vessels¹¹. The TAE treatment is highly dependent on the dispersion and integration of the embolization material. The experimental results showed that the application of PIB nanogels dispersion on right renal embolization was effective, uniform, and persistent. This phenomenon led to a significant drop in the right kidney volume and BF after embolization. BF, atrophy and calcification were observed in the right kidneys. The PIB nanogels remained in the blood vessel during the 12-week follow-up by evidence of pathologic examination. Zhao¹¹ studied the dispersion of the gel by different injection rates, while the long-term effect of the treatment was not observed by imaging methods and was unknown. In this study, we observed the dispersion of PIB in the right kidney and evaluated both the long-term effect of treatment by CT and pathology in a 12-week follow-up examination.

Assessing treatment efficacy is critical for any embolic material. In this experiment, we evaluated the embolization effect of the right renal artery using CT perfusion, a major advantage of which is non-invasion. In addition, this method can not only depict morphologic characteristics of the kidney but also provide additional quantitative factors that could influence the embolization effect. During follow-up, the volume of the right kidney decreased gradually after embolization, while the volume of the left kidney increased compensatively after the operation and then decreased slightly. After embolization of the right renal artery, the right renal BF decreased significantly to 0, and the left renal BF increased compensatively. The lack of vascular enhancement reflects necrosis and is regarded as successful treatment²⁶, demonstrating that the gelling agent has excellent permanency. The results of pathology further verify that the judgement of CT perfusion is correct, so evaluating the embolic effect is feasible by CT perfusion.

Nevertheless, there were some limitations to the current study. Not all the catheters are of good quality, and there were other personal factors. Moreover, the sample quantity was limited, the results were authentic yet still limited, and the sample quantity needs expanding to be compensated in a further study. In addition, we have not added chemotoxic agents to PIB to evaluate the rate of drug use. Studies regarding these properties of our new gel are now ongoing.

Conclusion

The effect of embolization on PIB was good, with good dispersion and permanency. The nanogel can reach the peripheral blood vessel and remain in it for a long time; thus, this gel is a good blood vessel embolic material and can be used in vivo. CT perfusion can be used to non-invasively and quantitatively evaluate the embolization effect of temperature-sensitive nanogels.

Declarations

Acknowledgements

We would like to thank all participants. Financial support: We acknowledge financial support from the National Natural Science Foundation of China (grant No. 81371661).

Competing Interests

The authors have declared that no competing interest exists.

Author contributions

All authors have contributed significantly in the content of the manuscript. P.H. and Y.Z. designed the study. Z.Z. and C.C. performed the experiments and wrote the manuscript. K.Q., H.L., X.Z. and H.Z. performed the experiments. G.M., Y.C., N.J. and C.Z. analyzed the data.

References

- 1 Kim, T. H. *et al.* Uterine artery embolization for primary postpartum hemorrhage. *Iranian journal of reproductive medicine*. **11**, 511-518 (2013).
- 2 Park, K. J. *et al.* Postpartum hemorrhage from extravasation or pseudoaneurysm: efficacy of transcatheter arterial embolization using N-butyl cyanoacrylate and comparison with gelatin sponge particle. *Journal of vascular and interventional radiology : JVIR*. **26**, 154-161, doi:10.1016/j.jvir.2014.10.001 (2015).
- 3 Urbano, J., Manuel Cabrera, J., Franco, A. & Alonso-Burgos, A. Selective arterial embolization with ethylene-vinyl alcohol copolymer for control of massive lower gastrointestinal bleeding: feasibility

and initial experience. *Journal of vascular and interventional radiology : JVIR*. **25**, 839-846, doi:10.1016/j.jvir.2014.02.024 (2014).

4 Li, Q. *et al.* Incidence and therapeutic frequency of extrahepatic collateral arteries in transcatheter arterial chemoembolization of hepatocellular carcinoma: Experience from 182 patients with survival time more than 3 years. *European journal of radiology*. **84**, 2555-2563, doi:10.1016/j.ejrad.2015.10.006 (2015).

5 Sun, C. J. *et al.* Transcatheter arterial embolization of acute gastrointestinal tumor hemorrhage with Onyx. *Indian journal of cancer*. **51 Suppl 2**, e56-59, doi:10.4103/0019-509x.151988 (2015).

6 Wang, B., Gao, B. L., Xu, G. P., Xiang, C. & Liu, X. S. Endovascular embolization is applicable for large and giant intracranial aneurysms: experience in one center with long-term angiographic follow-up. *Acta radiologica (Stockholm, Sweden : 1987)*. **56**, 105-113, doi:10.1177/0284185113520312 (2015).

7 Poyet, C., Grubhofer, F., Zimmermann, M., Sulser, T. & Hermanns, T. Therapy-resistant nephrolithiasis following renal artery coil embolization. *BMC urology*. **13**, 29, doi:10.1186/1471-2490-13-29 (2013).

8 Chen, W. J., Wang, S. C., Chen, S. L. & Kao, Y. L. Foreign body in the ureter: a particle of glue after transarterial embolization of a renal pseudoaneurysm during percutaneous nephrostomy. *Journal of the Chinese Medical Association : JCMA*. **75**, 183-186, doi:10.1016/j.jcma.2012.02.011 (2012).

9 Saba, R. *et al.* Pulmonary arterial hypertension secondary to ethanol sclerotherapy for renal artery embolization. *Case reports in critical care*. **2014**, 452452, doi:10.1155/2014/452452 (2014).

10 Bakar, B. *et al.* Evaluation of the toxicity of onyx compared with n-butyl 2-cyanoacrylate in the subarachnoid space of a rabbit model: an experimental research. *Neuroradiology*. **52**, 125-134, doi:10.1007/s00234-009-0594-8 (2010).

11 Zhao, H. *et al.* Temperature-sensitive poly(N-isopropylacrylamide-co-butyl methylacrylate) nanogel as an embolic agent: distribution, durability of vascular occlusion, and inflammatory reactions in the renal artery of rabbits. *AJNR Am J Neuroradiol*. **34**, 169-176, doi:10.3174/ajnr.A3177 (2013).

12 Zhao, Y. *et al.* Permanent and Peripheral Embolization: Temperature-Sensitive p(N-Isopropylacrylamide-co-butyl Methylacrylate) Nanogel as a Novel Blood-Vessel-Embolic Material in the Interventional Therapy of Liver Tumors. *Advanced Functional Materials*. **21**, 2035-2042, doi:10.1002/adfm.201002510 (2011).

13 Li, L. *et al.* Rational design of temperature-sensitive blood-vessel-embolic nanogels for improving hypoxic tumor microenvironment after transcatheter arterial embolization. *Theranostics*. **8**, 6291-6306, doi:10.7150/thno.28845 (2018).

- 14 Qian, K. *et al.* The studies about doxorubicin-loaded p(N-isopropyl-acrylamide-co-butyl methylacrylate) temperature-sensitive nanogel dispersions on the application in TACE therapies for rabbit VX2 liver tumor. *Journal of controlled release : official journal of the Controlled Release Society*. **212**, 41-49, doi:10.1016/j.jconrel.2015.06.013 (2015).
- 15 Cai, X. R. *et al.* Assessment of renal function in patients with unilateral ureteral obstruction using whole-organ perfusion imaging with 320-detector row computed tomography. *PloS one*. **10**, e0122454, doi:10.1371/journal.pone.0122454 (2015).
- 16 Ma, Y. *et al.* The studies on highly concentrated complex dispersions of gold nanoparticles and temperature-sensitive nanogels and their application as new blood-vessel-embolic materials with high-resolution angiography. *J Mater Chem B*. **2**, 6044-6053, doi:10.1039/C4TB00748D (2014).
- 17 Wan, J. *et al.* Doxorubicin-induced co-assembling nanomedicines with temperature-sensitive acidic polymer and their in-situ-forming hydrogels for intratumoral administration. *J Control Release*. **235**, 328-336, doi:https://doi.org/10.1016/j.jconrel.2016.06.009 (2016).
- 18 Zhao, H., Xu, J., Huang, W., Zhao, Y. & Yang, X. Thermosensitive Nanogels with Cross-Linked Pd(II) Ions for Improving Therapeutic Effects on Platinum-Resistant Cancers via Intratumoral Formation of Hydrogels. *Chemistry of Materials*. **31**, 5089-5103, doi:10.1021/acs.chemmater.9b00986 (2019).
- 19 Xiong, W. *et al.* Dual temperature/pH-sensitive drug delivery of poly(N-isopropylacrylamide-co-acrylic acid) nanogels conjugated with doxorubicin for potential application in tumor hyperthermia therapy. *Colloids and surfaces. B, Biointerfaces*. **84**, 447-453, doi:10.1016/j.colsurfb.2011.01.040 (2011).
- 20 Zhao, H. *et al.* Spatiotemporally Light-Activatable Platinum Nanocomplexes for Selective and Cooperative Cancer Therapy. *Acs Nano*. **13**, 6647-6661, doi:10.1021/acsnano.9b00972 (2019).
- 21 Wan, J. *et al.* Precise synchronization of hyperthermia–chemotherapy: photothermally induced on-demand release from injectable hydrogels of gold nanocages. *Nanoscale*. **10**, 20020-20032, doi:10.1039/C8NR06851H (2018).
- 22 Klouda, L. *et al.* Thermoresponsive, in situ cross-linkable hydrogels based on N-isopropylacrylamide: fabrication, characterization and mesenchymal stem cell encapsulation. *Acta biomaterialia*. **7**, 1460-1467, doi:10.1016/j.actbio.2010.12.027 (2011).
- 23 Akimoto, J. *et al.* Facile cell sheet manipulation and transplantation by using in situ gelation method. *Journal of biomedical materials research. Part B, Applied biomaterials*. **102**, 1659-1668, doi:10.1002/jbm.b.33148 (2014).
- 24 Shimizu, K., Fujita, H. & Nagamori, E. Oxygen plasma-treated thermoresponsive polymer surfaces for cell sheet engineering. *Biotechnology and bioengineering*. **106**, 303-310, doi:10.1002/bit.22677 (2010).

25 Mawad, D. *et al.* Synthesis and characterization of novel radiopaque poly(allyl amine) nanoparticles. *Nanotechnology*. **21**, 335603, doi:10.1088/0957-4484/21/33/335603 (2010).

26 Du, F., Jiang, R., Gu, M., He, C. & Guan, J. The clinical application of 320-detector row CT in transcatheter arterial chemoembolization (TACE) for hepatocellular carcinoma. *La Radiologia medica*. **120**, 690-694, doi:10.1007/s11547-015-0523-3 (2015).

Figures

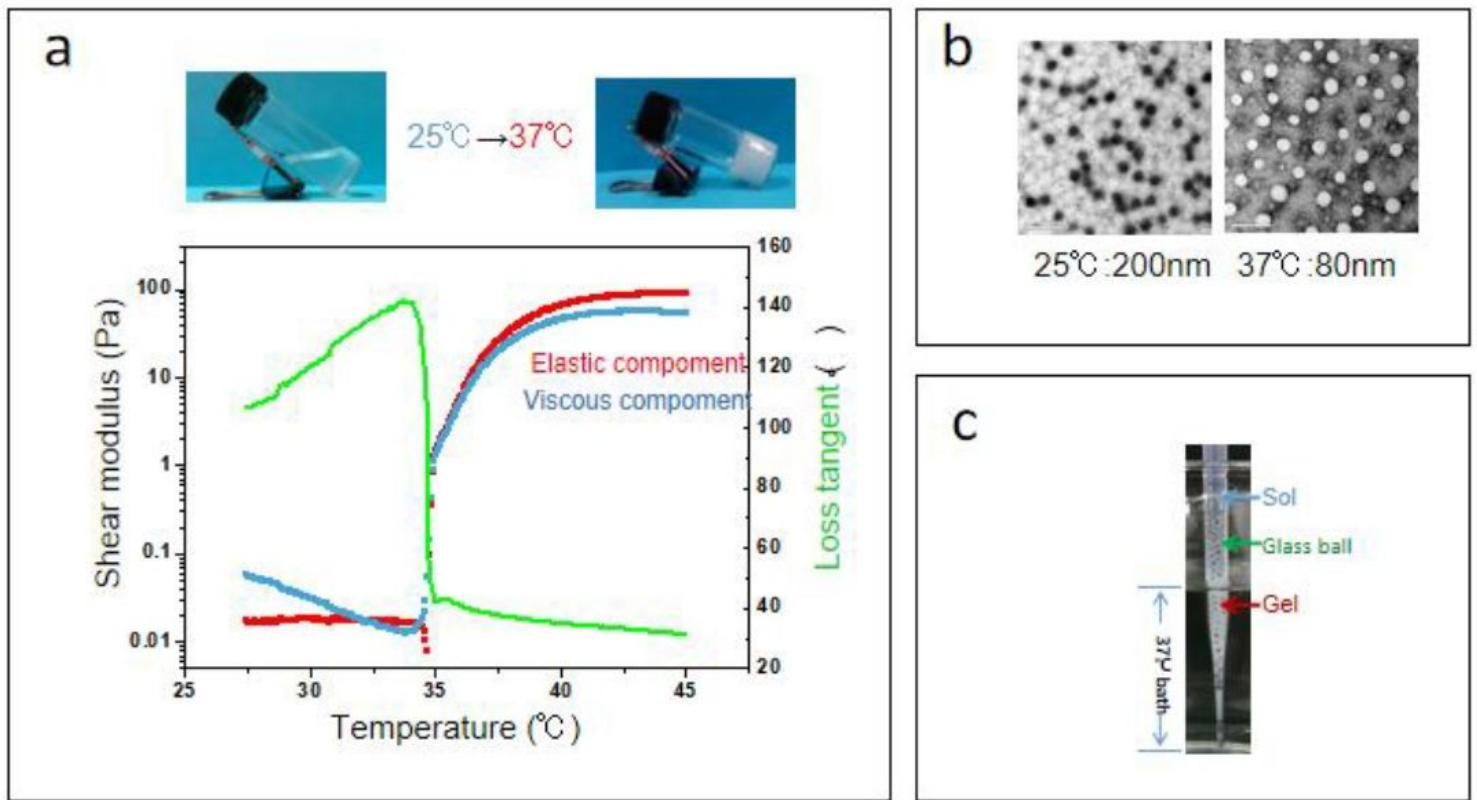


Figure 1

The temperature-sensitive PIB nanogel sol-gel phase-transition behaviors. (a) Temperature modulus testing found that the liquid-solid phase changed at 35 $^{\circ}\text{C}$; (b) TEM images showing the diameter of PIB nanogels at 25 $^{\circ}\text{C}$ and 37 $^{\circ}\text{C}$; (c) PIB nanogels were packed in a 2 mm diameter glass ball tube whose lower segment was immersed in a 37 $^{\circ}\text{C}$ constant temperature water bath; the liquid gel underwent phase transformation for a gel solid below the liquid level.



Figure 2

Right renal artery angiography of rabbits. (a) before embolization; (b) after embolization, white arrow indicates that the right renal artery is embolized.

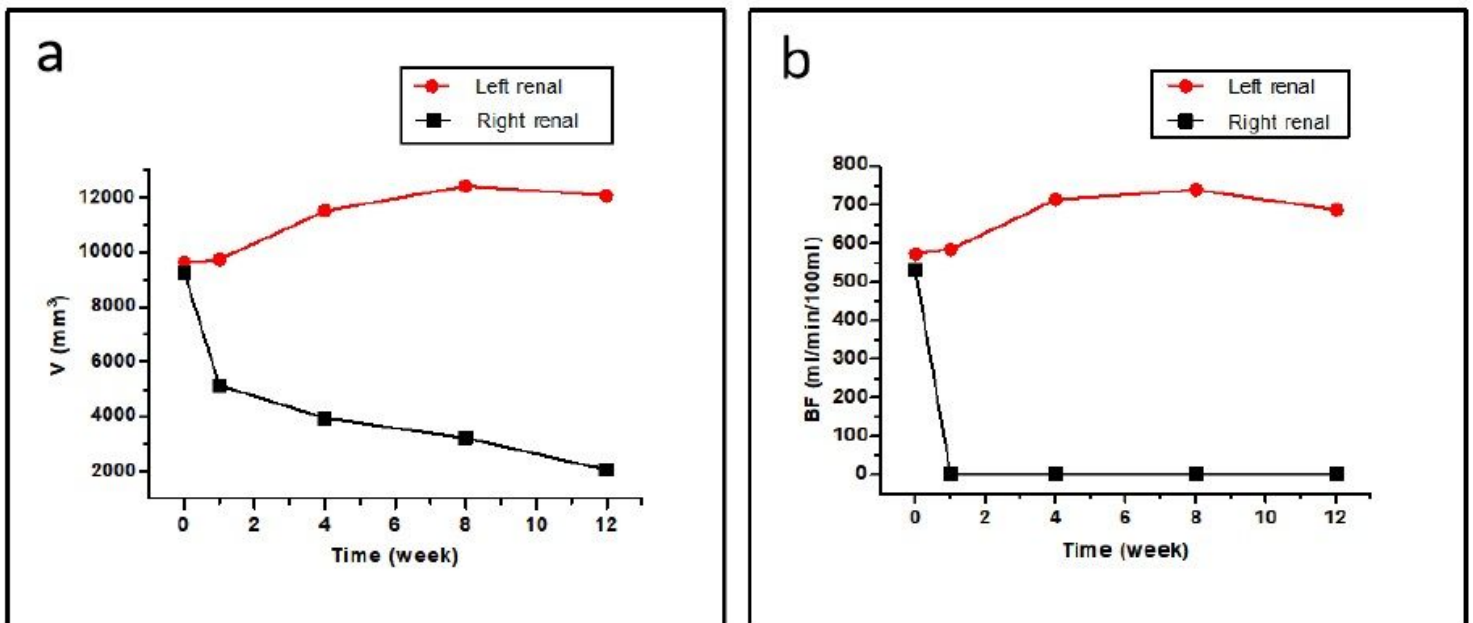


Figure 3

Morphological and haemodynamic changes of the two kidneys of a rabbit at different time points. (a) Changes in volume, individual renal volumes were measured by the ellipsoid formula (volume = length × width × thickness × $\pi/6$); (b) Changes in BF.

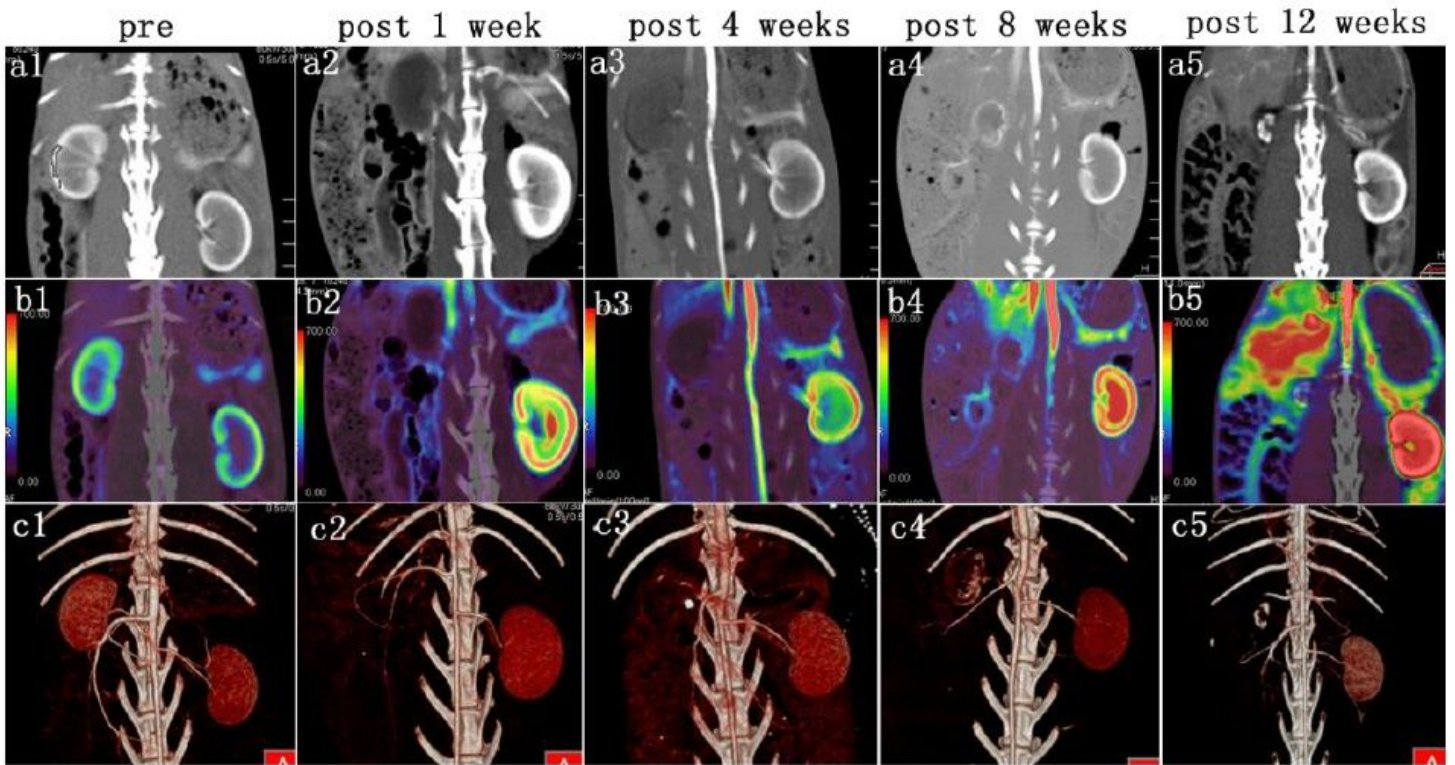


Figure 4

The images of CT examinations before and after embolization at different time. (a1-5) The enhanced images show significant shrinkage of the right kidney, with large calcifications. (b1-5) The perfusion maps show different colors of BF in the right kidney. (c1-5) The VRT images show significant calcification of the right kidney, but the left kidney and large blood vessels are clearly displayed.

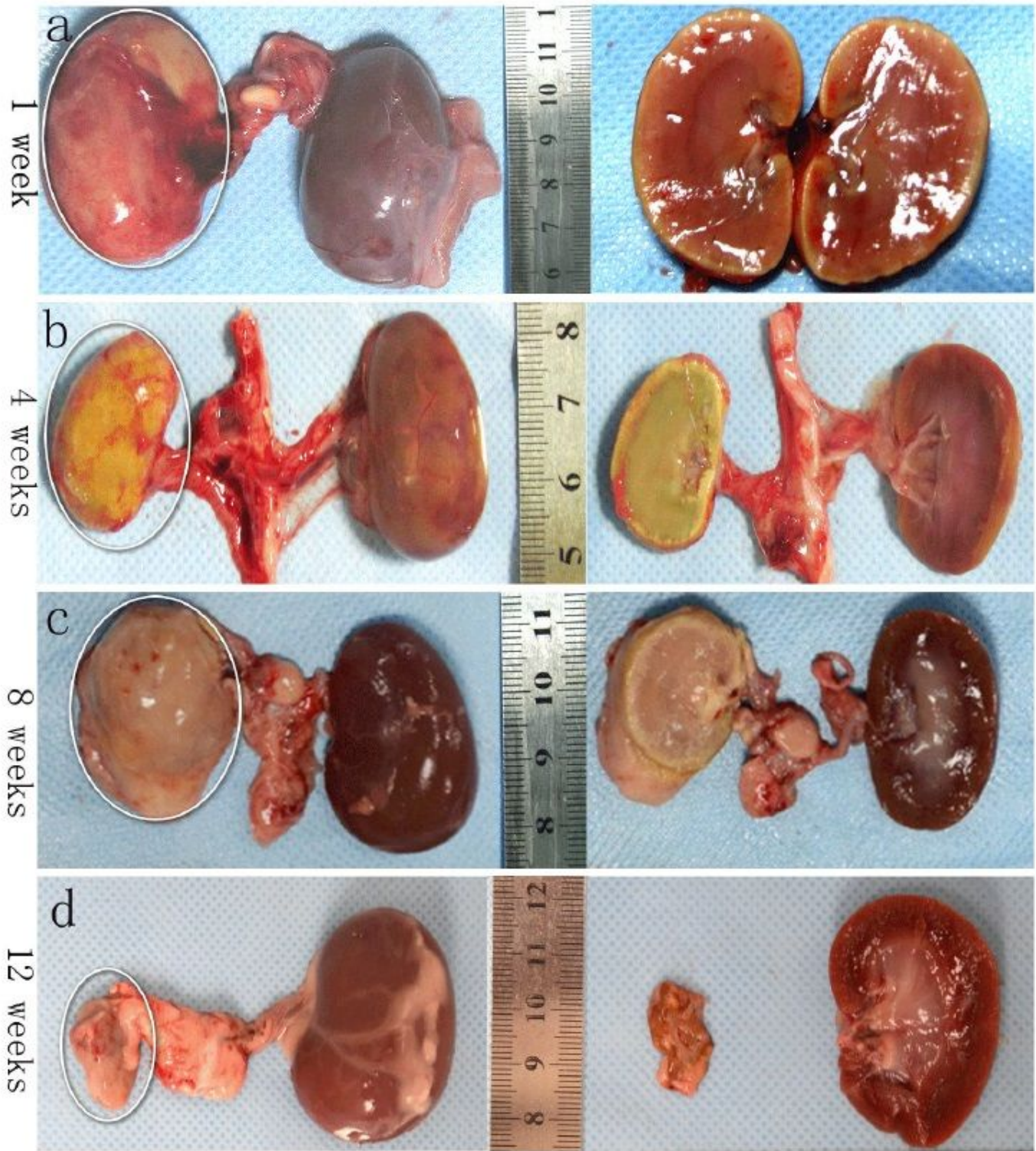


Figure 5

The macro-pathological pictures of the right kidneys of the rabbits after embolization at four different time points. (a-d) Pictures showed that the right kidney gradually shrank after embolization, combined with the compensatory enlargement of the left kidney.

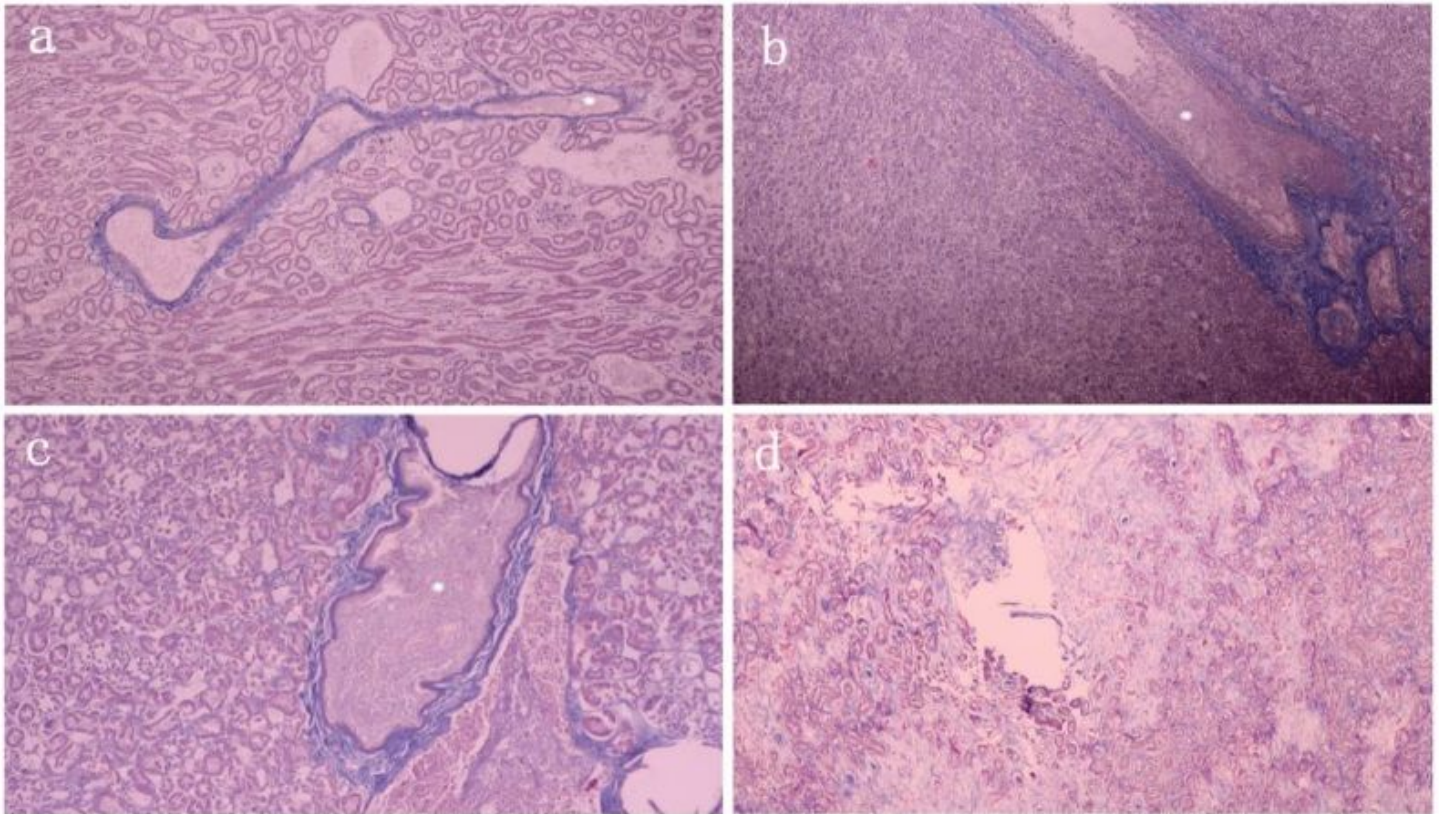


Figure 6

The representative pictures of Masson's trichrome of the kidney at different times after embolization. (a) One week after embolization: a few inflammatory cells around the vascular cavity and the solid gel are visible. (b and c) Four and eight weeks after embolization: without the formation of new blood vessels, the number of fiber cells increased. (*) indicates that the PIB nanogels remain in the blood vessel. (d) Twelve weeks after embolization: large amount of fibrous tissue hyperplasia; solid gel encapsulation by organization. (Original magnifications: 100 \times)